Available online at www.sciencedirect.com
SCIENCE DIRECT®
Journal of Solid State Chemistry 177 (2004) 1213–1218
JOURNAL OF SOLID STATE CHEMISTRY
http://elsevier.com/locate/jssc

Synthesis, characterization and magnetic properties of γ-Fe_2O_3 nanoparticles via a non-aqueous medium

Zhihong Jing[a,b] and Shihua Wu[a,*]

[a] Department of Chemistry, Nankai University, Tianjin 300071, China
[b] Department of Chemistry, Qufu Normal University, Qufu 273165, China

Received 7 July 2003; received in revised form 23 October 2003; accepted 29 October 2003

Abstract

Acicular shaped γ-Fe_2O_3 nanoparticles (major axis: 17 ± 2 nm; minor axis: 1.7 ± 1 nm) have been prepared using lauric acid as a non-aqueous medium. The products were investigated by IR, TG-DTA, XRD, Raman, SEM, TEM and magnetization measurements. For the preparation of pure γ-Fe_2O_3 nanoparticles, the suitable condition of the molar ratio of lauric acid to iron nitrate is set 2:1 and the appropriate temperature lies in the range 573–673 K. Besides, either pure α-Fe_2O_3 or a mixture of γ-Fe_2O_3 and α-Fe_2O_3 can also be obtained with the change of the molar ratio of lauric acid to iron nitrate. The experimental results indicate that the particle sizes, thermal stability and magnetic properties of the iron oxide strongly depend on the conditions in the preparation.

Keywords: γ-Fe_2O_3; Lauric acid; Non-aqueous medium; Magnetic property

1. Introduction

Over the past years, a lot of work has been done on the synthesis of γ-Fe_2O_3 particles due to their potential applications for ferrofluid, magnetic refrigeration, bio-processing, information storage and gas sensitive materials [1–7]. Considerable researches have been performed till now mainly on the preparation of γ-Fe_2O_3 particles in aqueous solution [8–10]. However, these products prepared from aqueous solution contained some inorganic ions such as Na^+ and Cl^-, which tend to be a major source of contamination of these particles [10]. Thus, non-aqueous solution approach has been employed to process γ-Fe_2O_3 nanoparticles due to the resultant precipitates being not contaminated. Particularly, Hyeon and co-workers [11] have successfully fabricated highly crystalline and monodisperse γ-Fe_2O_3 nanoparticles with a particle size of 13 nm by direct oxidation of iron pentacarbonyl in the presence of oleic acid with trimethylamine oxide as an oxidant. However, the synthesis of acicular γ-Fe_2O_3 nanoparticles, using lauric acid as a non-aqueous medium and $Fe(NO_3)_3\cdot9H_2O$ as starting precursor, has not been reported yet.

In order to prepare pure γ-Fe_2O_3 particles in a non-aqueous lauric acid medium, we present preliminary work in this paper, in which the suitable conditions have been found and detailed characterizations of the samples were done. In the preparation process, the precursors used are common and inexpensive compared with other methods.

2. Experimental

All the reagents were of analytical grade and used as received. A homogeneous solution was produced by addition of calculated amount of iron nitrate non-anhydrate $Fe(NO_3)_3\cdot9H_2O$ to a given amount of molten lauric acid. The molar ratio of lauric acid to iron nitrate was set at three different levels: 2:1 (S1), 1:1 (S2) and 1:2 (S3). The homogeneous solutions prepared with these compositions were heated separately in a beaker at 393 K with vigorous stirring till the evolution of brown gas (N_2O_5). A sticky moist red-brown mass was formed and cooled down to room temperature in air, then treated with 100 mL of tetrahydrofuran to form brown

*Corresponding author.
E-mail address: wushh@nankai.edu.cn (S. Wu).

0022-4596/$ - see front matter © 2003 Elsevier Inc. All rights reserved.
doi:10.1016/j.jssc.2003.10.034

precipitate which was collected by centrifugation and dried at 343 K in an air oven for 4 h. The yellow powders of the intermediate ferric oxide hydroxide (FeOOH) being essential to prepare γ-Fe_2O_3 particles were obtained.

IR spectra of the FeOOH and γ-Fe_2O_3 nanoparticles in KBr pellets were recorded in the range 4000–400 cm^{-1} on an American Nicolet AVATAR 380 FT-IR spectrometer. Thermal analyses were carried out on a ZRY-2P thermal analyzer by heating a 10 mg sample from room temperature to 973 K in air at a heating rate of 20 K min^{-1}. XRD spectra were performed on a Japan Rigaku D/max 2500 X-ray diffraction with Cu$K\alpha$ radiation ($\lambda = 1.5418$ Å). Raman spectra were collected in the range 4000–400 cm^{-1} on a Germany BRUKER FT-RAMAN spectrometer. The surface morphology was analyzed on a Japan HITACHI S-3500N scanning electron microscope. The particle size of the samples was determined on a Holland Phillips EM400ST transmission electron microscope. Magnetic measurements were carried out on an American LDJ 9600 vibrating sample magnetometer with a maximum field of 7.0 kOe at room temperature.

3. Results and discussion

The representative IR spectra of sample S1 (a) and sample S1 annealed at 573 K for 1 h (b) were shown in Fig. 1. As observed in Fig. 1a, the strong bands in the range 1700–1310 cm^{-1} could be assigned to the ionic nitrate (NO_3^-) [12–13], the 798 and 668 cm^{-1} peaks to the deformation vibration of Fe–OH groups and 3450–3200 cm^{-1} band to the stretching vibration of Fe–OH groups [14]. The small band near 2922 cm^{-1} was due to ν_s-CH_2 of residual lauric acid, suggesting the presence of FeOOH in the organic medium. However, in Fig. 1b, the peaks described above were disappeared and the characteristic IR spectra of γ-Fe_2O_3 particles appeared at 465, 585 and 632 cm^{-1} [1,2], respectively. This phenomenon indicated that the residual lauric acid and nitro compounds had decomposed and the FeOOH phase had transformed into γ-Fe_2O_3 completely after annealing at 573 K. It should be noted that the bands around 3430 and 1637 cm^{-1} in both samples were assigned to the stretching vibration of OH group and bending vibration of water molecules δ (HOH), respectively [15].

The IR spectra of samples S2 and S3 show similar trends, except that with the decrease of molar ratio of lauric acid to $Fe(NO_3)_3 \cdot 9H_2O$, the characteristic peaks of nitro compounds and ionic nitrate turn stronger.

The TG-DTA curves of sample S1 were shown in Fig. 2. The TG curve presents one step of thermal decomposition between 423 and 553 K with a weight loss of about 24.3% and no further changes beyond

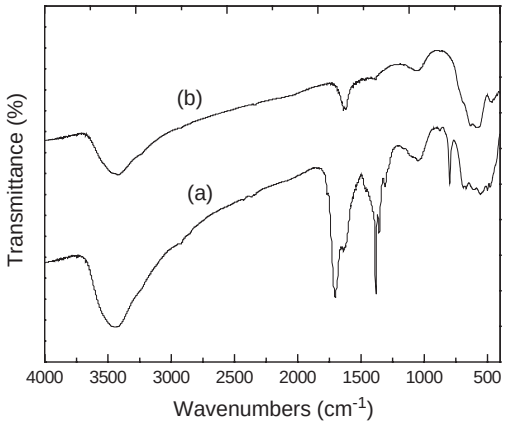

Fig. 1. IR spectra of (a) sample S1, and (b) sample S1 annealed at 573 K for 1 h.

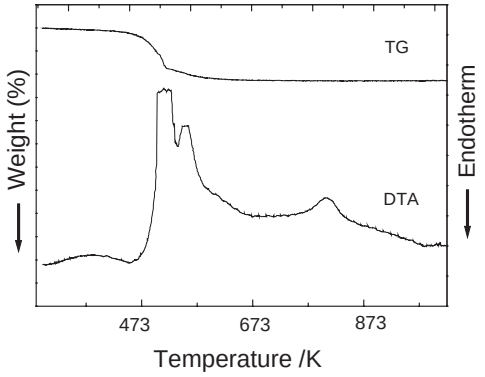

Fig. 2. TG-DTA curves of sample S1.

573 K were observed. This could be ascribed to the removal of water and the residual lauric acid. The DTA curve includes four main steps of thermal decomposition. The first step between 433 and 473 K is accompanied by an endothermal effect which is assigned to water desorbtion and the release of attached nitrogen compounds. The other three steps are accompanied by exothermal effects which are assigned to the combustion of lauric acid between 473 and 538 K, the crystallization of amorphous FeOOH particles along with partial γ-Fe_2O_3 formation between 538 and 653 K, and the transformation of γ-Fe_2O_3 phase into more stable α-Fe_2O_3 particles in the range 773–873 K, respectively. The TG-DTA curves of samples S2 (Fig. 3) and S3 (Fig. 4) presented similar trends except several slight differences.

XRD patterns of samples S1, S2 and S3 annealed at different temperatures for 1 h were showed in Figs. 5, 7 and 8, respectively. From Fig. 5, the X-ray patterns can compare well with standard γ-Fe_2O_3 reflections when heated at 573 K (a) and 673 K (b). In particular, the maghemite peak is slightly sharper in (a) than that in (b), and the average size of the samples shown in (a) and (b) calculated from the half-width of the diffraction peaks

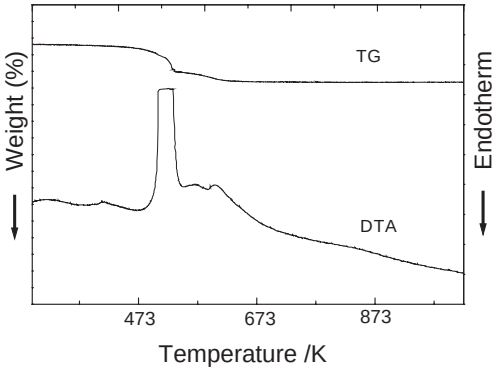

Fig. 3. TG-DTA curves of sample S2.

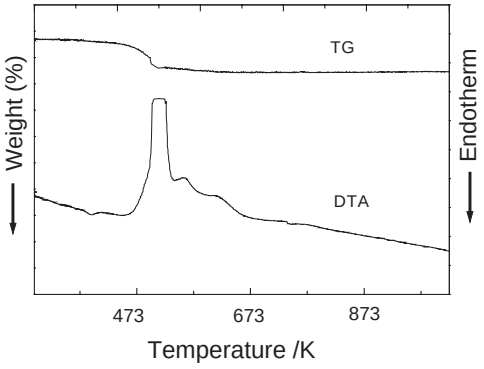

Fig. 4. TG-DTA curves of sample S3.

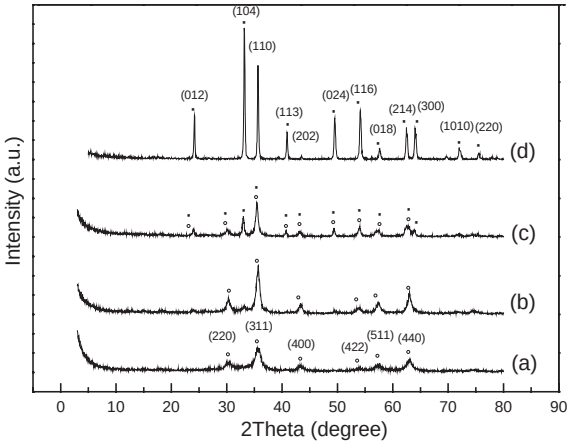

Fig. 5. XRD patterns of sample S1 annealed at different temperatures: (a) 573 K, (b) 673 K, (c) 773 K, and (d) 973 K (where (●) = α-Fe_2O_3, (○) = spinel structure).

(using Scherrer's equation) are 8 and 13.8 nm, respectively. As expected, the average crystallite size of γ-Fe_2O_3 particles increased with the raise in annealing temperatures. When temperature rose up to 773 K, a small amount of α-Fe_2O_3 was detected and the phase was a mixture of maghemite (γ-Fe_2O_3) and hematite (α-Fe_2O_3). Above 973 K, γ-Fe_2O_3 would be completely transformed into α-Fe_2O_3 whose average size was 18 nm. Compared with standard Fe_3O_4 and γ-Fe_2O_3 XRD data, the two peaks at 2θ angle of 35.5° and 62.7° could be attributed to either Fe_3O_4 or γ-Fe_2O_3 (311) and (440) peaks.

In order to distinguish the Fe_3O_4 and γ-Fe_2O_3, Raman spectra were further performed. As shown in Fig. 6, Raman spectra for sample S1 annealed at 573 and 673 K for 1 h all showed two peaks, centered at the wavelength of around 1370 and 1580 cm^{-1}, respectively, which could be attributed to γ-Fe_2O_3 phase. At the same time, the broadened peak over the wavelength 600–800 cm^{-1} was also a characteristic band of γ-Fe_2O_3 [16], which further confirms that the spinel phase is γ-Fe_2O_3, not Fe_3O_4.

As observed from Fig. 7, when heating sample S2 at 573 K (a), γ-Fe_2O_3 crystalline peaks appeared, when temperature rose up to 673 K (b), two phases (γ-Fe_2O_3 and α-Fe_2O_3) were presented simultaneously, and above 773 K (c), the phase identification revealed the characteristic pattern of γ-Fe_2O_3.

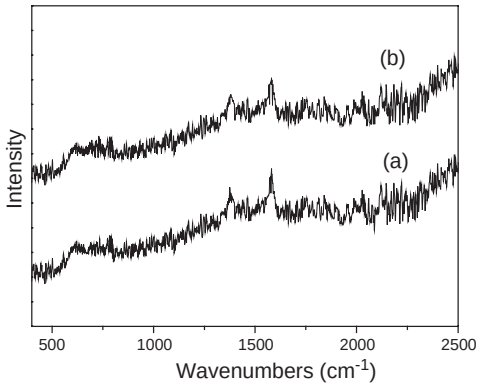

Fig. 6. Raman spectra of sample S1 annealed at (a) 573 K for 1 h, and (b) 673 K for 1 h.

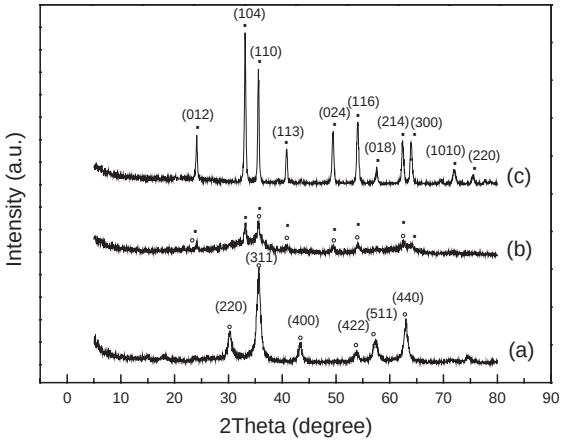

Fig. 7. XRD patterns of sample S2 annealed at different temperatures: (a) 573 K, (b) 673 K, and (c) 773 K (where (●) = α-Fe_2O_3, (○) = spinel structure).

As shown from Fig. 8, when sample S3 was heated at 573 (a) and 673 K (b), the XRD pattern exhibits a mixture of γ-Fe_2O_3 and α-Fe_2O_3. Above temperature 773 K (c), γ-Fe_2O_3 would be transformed into α-Fe_2O_3 completely. The main reason for the presence of the mixture phase was that the residual $Fe(NO_3)_3 \cdot 9H_2O$ transformed into α-Fe_2O_3 directly when heated at 573 K, indicating that the molar ratio of lauric acid to iron nitrate was unsuitable for preparation of pure γ-Fe_2O_3.

The XRD results of samples S1, S2 and S3 annealed at different temperatures for 1 h were given in Table 1. From Table 1, it was clear that either pure γ-Fe_2O_3, or pure α-Fe_2O_3, or a mixture of γ-Fe_2O_3 and α-Fe_2O_3 could be easily obtained by changing the annealing temperatures and molar ratio of iron nitrate to lauric acid. And sample S1 was the better selection to be used as magnetic materials due to its high crystallinity without any phase impurity. Hence, in this paper, we select sample S1 annealed at different temperatures for further characterization by SEM and TEM.

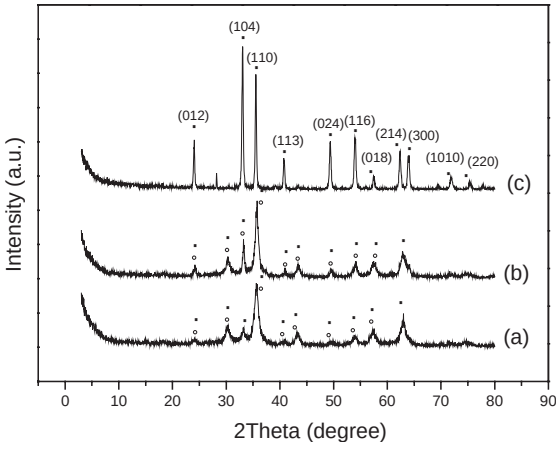

Fig. 8. XRD patterns of sample S3 annealed at different temperatures: (a) 573 K, (b) 673 K, and (c) 773 K (where (●) = α-Fe_2O_3, (○) = spinel structure).

The SEM pictures of sample S1 annealed at 673 and 973 K were shown in Figs. 9a and b, respectively. As seen from Fig. 9a, a lot of globular clusters along with acicular shape bars of γ-Fe_2O_3 are observed, indicating that the γ-Fe_2O_3 particles are agglomerated. When the annealing temperature increases to 873 K, the surface of globular clusters becomes much rougher and the acicular shape bars become shorter evidently, suggesting that the morphology of γ-Fe_2O_3 and α-Fe_2O_3 is different from each other. The results would be further verified by following TEM studies.

The TEM photographs of sample S1 annealed at 673 and 973 K were shown in Figs. 10a and b, respectively. In Fig. 10a, slender acicular shaped γ-Fe_2O_3 nanoparticles are observed with major axis: 17 ± 2 nm; minor axis: 1.7 ± 1 nm. While in Fig. 10b, cylindrical shaped α-Fe_2O_3 nanoparticles are seen with major axis: 15 ± 1 nm; minor axis: 3.5 ± 1 nm.

It is known that acicular shaped γ-Fe_2O_3 nanoparticles possess better magnetic property [1]. So only the magnetic characterization has been done with the acicular shaped γ-Fe_2O_3, in which sample S1 annealed

Table 1
X-ray diffraction analysis results of the samples annealed at different temperatures

Sample	Molar ratio	Annealed temperature (K) and phase composition			
		573	673	773	973
S1	2:1	γ-Fe_2O_3	γ-Fe_2O_3	γ-Fe_2O_3 + α-Fe_2O_3	α-Fe_2O_3
S2	1:1	γ-Fe_2O_3	γ-Fe_2O_3 + α-Fe_2O_3	α-Fe_2O_3	
S3	1:2	γ-Fe_2O_3 + α-Fe_2O_3	γ-Fe_2O_3 + α-Fe_2O_3	α-Fe_2O_3	

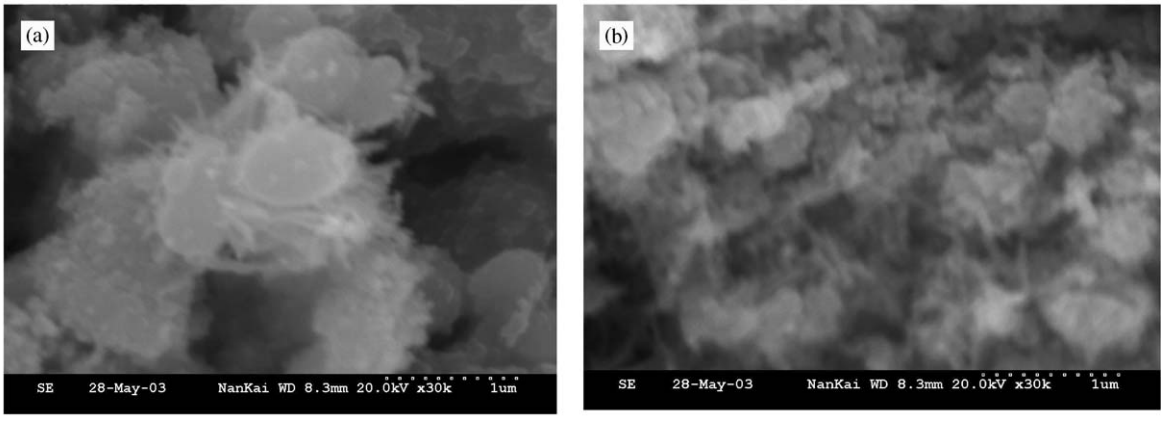

Fig. 9. SEM pictures of sample S1 annealed at: (a) 673 K, and (b) 973 K.

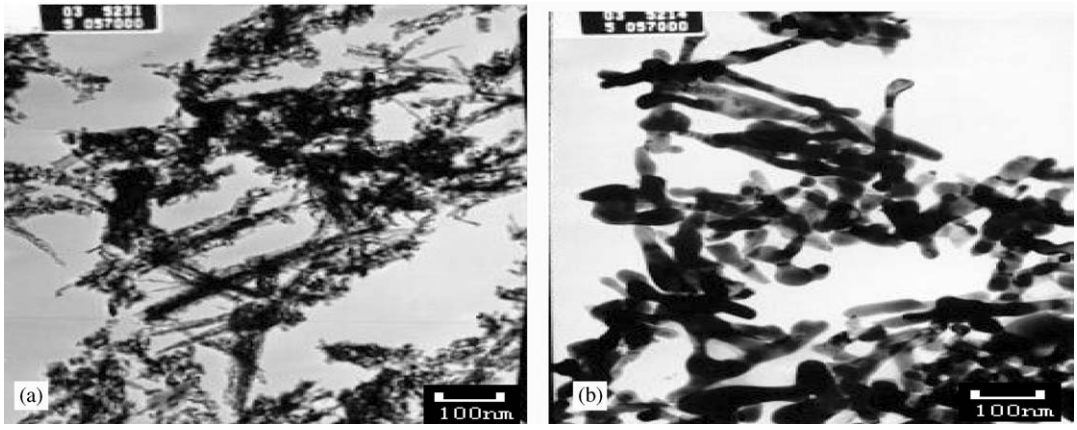

Fig. 10. TEM photographs of sample S1 annealed at: (a) 673 K, and (b) 973 K.

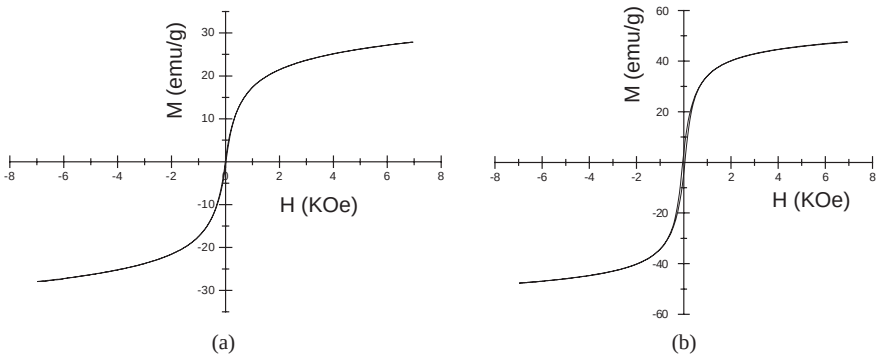

Fig. 11. Hysteresis loops of sample S1 annealed at: (a) 573 K, and (b) 673 K.

at 573 and 673 K temperature was done at room temperature and the hysteresis loops were made with a field scan of ± 7.0 kOe. The results were shown in Figs. 11a and b. From Figs. 11a and b, for sample S1 annealed at 573 K, the saturation magnetization (M_s), remnant magnetization (M_r), coercivity (H_c), and squareness (M_r/M_s) were determined to be 27.99, 0.5753 emu/g, 11.08 Oe, and 0.021, respectively; while for sample S1 annealed at 673 K, the corresponding values were determined to be 47.68, 4.023 emu/g, 45.33 Oe, and 0.084, respectively. It is obviously that the corresponding values of the former are lower than those of the latter due to its smaller particles. However, the saturation magnetization of the γ-Fe_2O_3 nanoparticles obtained is much lower than that of the bulk γ-Fe_2O_3 (76 emu/g) [17], which probably could be attributed to the nanoscale dimension and the surface effects [18]. In addition, whether there are other factors that could influence the saturation magnetization of these particles is still an open question yet.

4. Conclusions

In this work, acicular shaped γ-Fe_2O_3 nanoparticles (major axis: 17 ± 2 nm; minor axis: 1.7 ± 1 nm) have been prepared using lauric acid as a non-aqueous medium and $Fe(NO_3)_3 \cdot 9H_2O$ as starting precursor. To prepare acicular shaped pure γ-Fe_2O_3 nanoparticles in the non-aqueous medium, the suitable molar ratio of lauric acid to iron nitrate is set 2:1 and the appropriate temperature is in the range of 573–673 K. In addition, it is shown by XRD analysis that either pure α-Fe_2O_3 or a mixture of γ-Fe_2O_3 and α-Fe_2O_3 nanoparticles can also be easily obtained by changing the annealing temperatures and molar ratio of iron nitrate to lauric acid for various needs. The smaller dimension and better stability are caused by lauric acid, which hinders the increasing of the dimension and favors the formation of γ-Fe_2O_3 nanoparticles. Hence, we postulate that it would be a promising technique for preparation of nanoscale metal oxides in non-aqueous systems using lauric acid as medium. It should be pointed out that the reason, why the saturation magnetization of the obtained γ-Fe_2O_3 nanoparticles is lower compared with other methods, is still under way.

References

[1] V. Chhabra, P. Ayyub, S. Chattopadhyay, A.N. Maitra, Mater. Lett. 26 (1996) 21.

[2] T. Gonzalez-Carreno, A. Mifsud, J.M. Palacios, C.J. Serna, Mater. Chem. Phys. 27 (1991) 287.
[3] K. Suresh, K.C. Patil, J. Mater. Sci. Lett. 12 (1993) 572.
[4] Y.S. Kang, S. Risbud, J.F. Rabolt, P. Stroeve, Chem. Mater. 8 (1996) 2209.
[5] W. Chang, M. Deng, T. Tsai, T. Ching, Jpn. J. Appl. Phys. 31 (1992) 1343.
[6] D. Li, X. Wang, X. Wang, J. Mater. Sci. Lett. 6 (1997) 493.
[7] M. Liao, D. Chen, J. Mater. Chem. 12 (2002) 3654.
[8] B.R.V. Narasimban, S. Prabhakar, Mater. Lett. 52 (2002) 295.
[9] M.P. Morales, M.A. Verges, J. Magn. Magn. Mater. 203 (1999) 146.
[10] Y. Konoshi, T. Kawamura, S. Asai, Ind. Eng. Chem. Res. 32 (1993) 2888.
[11] T. Hyeon, S.S. Lee, J. Park, J. Am. Chem. Soc. 123 (2001) 12798.
[12] C. Camypeyret, J.M. Flaud, L. Lechueafossat, Chem. Phys. Lett. 139 (1987) 345.
[13] K. Nakajima, Y. Hirotsu, S. Okamoto, J. Am. Ceram. Soc. 70 (1987) 321.
[14] A. Miiller, Arzeinmitted Forsch. 17 (1967) 921.
[15] A. Jitianu, M. Crisan, A. Meghea, I. Rau, M. Zaharescu, J. Mater. Chem. 12 (2002) 1401.
[16] D.L.A.D. Faria, S.V. Silva, M.T.D. Oliveira, J. Raman Spectrosc. 28 (1997) 873.
[17] B.D. Cullity, Addison-Wesley, Reading, MA, 1972, 201pp.
[18] L. Asenjo, J. Tejada, Appl. Phys. A 74 (2002) 591.